BMC Microbiology

RESEARCH

Open Access

Lactiplantibacillus plantarum extracellular vesicles exert anti-PEDV effects through STING-dependent autophagy

Shihan Zhang[1,2,3], Xin Shan[1,2,3], Guanglong Qu[1,2,3], Anqi Sun[1,2,3], Junhong Xing[1,2,3], Qiuyuan Liu[3], Zixuan Liu[2,3], Yibing Wang[2,3], Xinyue Zhang[1,2,3], Xin Cao[1,2,3], Yan Zeng[1,2,3], Jianzhong Wang[1,2,3], Chunfeng Wang[1,2,3*] and Jingtao Hu[1,2,3*]

Abstract

Porcine epidemic diarrhea virus (PEDV) infection causes severe gastrointestinal and lethal disease in piglets, leading to huge economic losses for the swine industry worldwide. Recent studies have emphasized probiotics can regulate innate immunity and cellular functions through interaction with intestinal epithelial cells via extracellular vesicles (EVs) as effective carriers. The cGAS-STING signaling pathway is crucial for inducing type I interferons (IFNs) to establish antiviral innate immunity. It also triggers cellular autophagy, which helps maintain intracellular environmental homeostasis. In our study, we found that *Lactiplantibacillus plantarum* extracellular vesicles (LpEVs) significantly activated the cGAS-STING signaling pathway in porcine intestinal epithelial cells (IPEC-J2), thereby enhancing antiviral immune responses. Notably, compared to the untreated control group, 10 μg/mL LpEVs retained the capacity to activate the cGAS-STING pathway, but their activation efficacy was significantly lower than that of 2.5 μg/mL, suggesting a potential feedback regulatory mechanism at higher concentrations. Furthermore, 10 μg/mL LpEVs regulated cGAS-STING activation through autophagy induction, and this autophagic response was STING-dependent. Additionally, LpEVs at concentrations of 2.5, 5, and 10 μg/mL all significantly inhibited the proliferation of PEDV. However, 10 μg/mL LpEVs exhibited a stronger inhibitory effect on PEDV replication compared to 2.5 or 5 μg/mL doses, and this enhanced antiviral activity was closely associated with autophagy. Our findings elucidate the underlying mechanism of antiviral effects of probiotics through regulating innate immunity and autophagy, which highlights the critical role of LpEVs in preventing PEDV infection as a potential antiviral agent.

Keywords *Lactiplantibacillus plantarum*, Extracellular vesicles, Autophagy, STING, PEDV

Introduction

Orcine epidemic diarrhea virus (PEDV), a member of the *Alphacoronavirus* genus within the *Coronaviridae* family, causes acute diarrhea, vomiting, dehydration, and high mortality in neonatal piglets [1]. Over the past 30 years, numerous reports have documented the global impact of porcine epidemic diarrhea, which has caused substantial economic losses in the swine industry due to the absence of effective drugs or vaccines [2]. Therefore, it is urgent to develop novel and efficient antiviral strategies to prevent PEDV infection.

*Correspondence:
Chunfeng Wang
wangchunfeng@jlau.edu.cn
Jingtao Hu
jingtaoh@jlau.edu.cn
[1] Engineering Research Center of Microecological Vaccines (Drugs) for Major Animal Diseases, Ministry of Education, Changchun 130118, China
[2] Animal Medical College, Jilin Agricultural University, Changchun 130118, China
[3] College of Animal Science and Technology, Jilin Agricultural University, Changchun 130118, China

Lactobacillus, a characterized probiotic with well-documented health benefits, has emerged as a potent antiviral agent demonstrating efficacy against diverse viral pathogens. Growing literatures have elucidated multiple mechanisms underlying its antiviral effects: direct virucidal effects via surface adhesins and antimicrobial peptides; modulation of innate immune responses through signaling pathway (e.g., TLR/NF-κB) regulation; and production of bioactive metabolites that impair viral replication cycles [3–5]. Emerging mechanistic studies further reveal strain-specific antiviral signatures dependent on bacterial-epithelial cell crosstalk. How these strains translocation across the host barrier to communicate with distal cells and impact viral infections remains elusive. Type I interferons (IFN-I) play a crucial role in antiviral immunity. Emerging evidence has demonstrated that probiotics-derived extracellular vesicles (EVs) serve as critical mediators of host-microbe crosstalk by trafficking immunogenic cargo during IFN priming. Notably, *Lactobacillus* extracellular vesicles have been shown to activate the cyclic GMP-AMP synthase-stimulator of interferon genes (cGAS-STING) pathway through delivering bacterial DNA to distant host cells [6, 7]. This EVs-mediated"defense priming"mechanism suggests a sophisticated evolutionary strategy where commensal microbes remotely regulate host immunity response against viral invaders. Systematic comparisons reveal that extracellular vesicles exhibit enhanced immunoregulatory capacity relative to crude bacterial preparations in regulating intestinal immune cell response and fortifying epithelial barrier integrity [8–10].

The cGAS-STING-IFN-I signaling axis serves as a central mechanism in antiviral defense [11, 12]. Upon detection of cytosolic microbial DNA, cyclic GMP-AMP synthase (cGAS) catalyzes the synthesis of the cyclic dinucleotide 2′3′-cGAMP. This second messenger binds to STING at the endoplasmic reticulum (ER), inducing its translocation and subsequent recruitment of TBK1. Activated TBK1 phosphorylates IRF3 to initiate IFN-I production and downstream interferon-stimulated gene (ISG) expression, which establish an antiviral cellular state[13, 14]. However, dysregulated hyperactivation of this pathway is increasingly linked to tissue inflammation and organ pathology [15]. Accumulating evidence indicates that the cGAS-STING pathway has been shown to induce the autophagy pathway, a conserved lysosomal degradation system, through non-canonical mechanisms [16, 17]. Mechanistic studies demonstrate that STING directly engages microtubule-associated protein 1 light chain 3 (LC3) via LC3-interacting region (LIR) motif, thereby autophagosome formation [18]. Interestingly, STING activation triggers autophagy in a TBK1/IRF3-independent manner but requires core autophagy proteins including ATG5, ATG16L1, and ATG7 [18, 19].

Autophagy selectively targes long-lived proteins and dysfunctional organelles for lysosomal degradation and subsequent recycling of cellular components [20, 21]. This evolutionarily conserved mechanism acts as a critical cellular stress adaptor, enabling dynamic homeostasis maintenance under diverse pathological challenges [22, 23]. Mechanistic studies reveal that the autophagy-related protein Beclin-1 binds and inhibits cGAS, thereby blocking downstream IFN-I production. Simultaneously, this interaction activates autophagy-mediated clearance of cytoplasmic DNA to restore cellular equilibrium [15]. Furthermore, autophagy enhances the degradation of STING itself-degradation, thereby suppressing IFN production and apoptosis to promote homeostasis restoration [24]. Accumulating studies demonstrate autophagy is capable of inhibiting viral replication through multiple mechanisms [25, 26]. For example, host protein RNA-binding motif protein 14 (RBM14) recruits the cargo receptor p62 via the RBM14-p62-autophagosome axis to degrade PEDV nucleocapsid (N) protein [27]. Zinc ions (Zn^{2+}) similarly suppress PEDV replication in Vero E6 cells by inducing autophagy [28]. Notably, deficiency in autophagy-related protein ATG5 significantly impairs IFN-α production triggered by viral pathogens, including vesicular stomatitis virus (VSV), Sendai virus, influenza virus, HIV-1, and herpes simplex virus (HSV) [29]. These evidences highlight autophagy as a key process for viral sensing and initiation of antiviral immune responses.

In this study, we investigated the antiviral efficacy of *Lactiplantibacillus plantarum*-derived extracellular vesicles (LpEVs) against PEDV in intestinal epithelial cells (IPEC-J2), focusing on the mechanistic crosstalk between cGAS-STING pathway and autophagy. Our findings revealed that LpEVs potently activated the cGAS-STING pathway, induced autophagic through STING-dependent mechanisms, and establish a self-regulatory circuit where autophagy exerted negative feedback to attenuate cGAS-STING excessive activation. Notably, STING-mediated autophagy triggered by LpEVs exhibited synergistic enhancement of antiviral efficacy. This study establishes a novel framework for developing EVs-based antiviral strategies targeting pathogen-immune interplay.

Materials and methods

Cells and viruses

IPEC-J2 cells (ACC 701) were purchased from DMSZ (Braunschweig, Germany) and cultured in Dulbecco's modified Eagle's medium/Nutrient Mixture F-12 (DMEM/F12) (Sevenbio, Beijing, China) supplemented with 10% fetal bovine serum (FBS) (Sangon, Shanghai) with penicillin (100 U/ml)/streptomycin (100 mg/

ml) (Sevenbio, Beijing, China). All cultures were maintained in a humidified incubator at 37 °C with 5% CO_2. The strain of the porcine epidemic diarrhea virus (PEDV) (CV777) was stored in our laboratory.

Chemical reagents and antibodies

The 2× SYBR Green qPCR MasterMix II (Universal) and the All-in-one First Strand cDNA Synthesis Kit II (with dsDNase) for quantitative PCR were purchased from Seven Biotechnology Co., Ltd (Beijing, China). The following monoclonal antibodies (mAb) were provided by ABclonal (Wuhan, China): LC3B rabbit mAb (A19665), SQSTM1/p62 rabbit mAb (A19700), STING/TMEM173 rabbit mAb (A21051), and cGAS rabbit mAb (AB335). Additionally, AdPlus-mCherry-GFP-LC3B(C3012), IRF3 rabbit mAb (AF2485), Phospho-IRF3 (Ser386) rabbit mAb (AF1594), FITC-labeled goat anti-rabbit IgG (H +L) (A0562), GAPDH mouse mAb (AF1186), and β-actin rabbit mAb (AF5003) were all obtained from Beyotime Institute of Biotechnology (Shanghai, China). 3-methyladenine (3-MA) (HY-19312) and STING-IN-2 (C-170) (HY-138682) were purchased from MedChemExpress LLC (Shanghai, China). PEDV nucleoprotein mAb (M100048) was purchased from Zoonogen Biotechnology Co., Ltd (Beijing, China).

Strain and purification of EVs

Lactiplantibacillus plantarum JL01 (CGMCC No. 18056), originally isolated from the intestinal content of piglets in our previous study [30], was anaerobically cultured in MRS broth (Difco, USA; Catalog No. DF0881-17–5) at 37 °C overnight. LpEVs were isolated from the culture supernatants using ultrafiltration combined with ultracentrifugation. In brief, the culture supernatants were collected by centrifugation (8,000 rpm, 15 min, 4 °C) to remove cell debris and impurities, and then were filtered through a 0.22 μm filter (Merck Millipore, USA). The supernatant was concentrated using 10 kDa MWCO concentrators (3,000 rpm, 30 min, 4 °C) twice and ultracentrifuged at 100,000 ×g (4 °C) for 2 h. The precipitate was resuspended with PBS and ultracentrifuged at the same condition again, finally resuspended the pellet with PBS and storage at −80 °C. Total protein content was determined by Bradford assay (Bio-Rad, USA). The morphology and the size distribution of LpEVs were observed by transmission electron microscope (TEM) (JEM-F200, Jeol Ltd., Japan) and nanoparticle tracking analysis (NTA) (Zetaview-PMX120-Z, Particle Metrix Inc., Germany).

Detection of cell viability by CCK-8

IPEC-J2 cells (1×10^5 cells/well) seeded in 96-well plates were treated with varying concentration of LpEVs (2.5, 5, 10, and 20 μg/mL) for 12 h. Additionally, a fixed dose was administered for 3, 6, 9, and 12 h, respectively. The culture medium was then replaced with a 100 μL DMEM/F12 medium containing 10 μL of CCK-8 reagent (Beyotime, Shanghai, China) and incubated at 37 °C for 1 h. The optical density (OD) was measured at 450 nm by a microplate reader (Biotek HTX, Beijing, China). Cell viability was evaluated as (OD value of the stimulated cell-OD value of unstimulated cells)/(OD value of the unstimulated cell-OD value of blank) ×100%.

ELISA

IPEC-J2 cells (5×10^5) were seeded in 6-well plate and treated with varying concentrations of LpEVs (2.5, 5, and 10 μg/mL) for 12 h. The cell culture supernatant was collected by centrifugation (1500 rpm, 15 min, 4 °C). The supernatant was quantified using IFN-α and IFN-β ELISA detection kit (Meimian Biotechnology, Jiangsu, China) according to the manufacturer's protocols. Absorbance was measured at 450 nm using a microplate reader (Biotek HTX, Beijing, China).

qPCR

Total RNA was extracted from IPEC-J2 cells (1×10^6) treated with LpEVs (2.5, 5, 10 μg/mL) for 12 h in 6-well plate using TRIzol® reagent (Takara, Japan) following standard protocols. cDNA synthesis was performed with the First Strand cDNA Synthesis Kit (Sevenbio, China). Quantitative PCR reactions utilized SYBR Green MasterMix (Sevenbio) on an Applied Biosystems 7500 Real-Time PCR System. The results are displayed as relative expression values normalized to that of GAPDH. Relative gene quantification was calculated using the $2^{-\Delta\Delta Ct}$ method. The specific primer sequences are provided in the Table 1.

Western blotting

Total proteins were extracted from IPEC-J2 cells (1×10^6) treated with LpEVs (2.5, 5, 10 μg/mL) for 12 h using RIPA lysis buffer (Beyotime Institute of Biotechnology, Shanghai, China). The protein concentrations in the lysates were quantified and adjusted using a BCA protein assay kit (Beyotime, Shanghai, China). The protein samples were then mixed with 4× loading buffer in a 3:1 ratio and heated at 95 °C for 10 min. The protein supernatant was subjected to SDS-PAGE and subsequently transferred to a PVDF membrane. The membrane was blocked with 5% nonfat milk at room temperature for 2 h and then incubated with the primary antibody (including LC3B, SQSTM1/p62, STING/TMEM173, cGAS, IRF3, Phospho-IRF3, β-actin, GAPDH, and PEDV nucleoprotein mAb) overnight at 4 °C. After washing with TBST, the membrane was incubated with a secondary antibody (GAPDH and β-actin mAb) at room temperature

Table 1 Primers for qPCR amplification used in this study

Gene	Primer set	Sequence (5′–3′)
IFN-α	Forward	CTGGCCAACCTGCTCTCTAG
	Reverse	CTCCTGCGGGAATCCAAAGT
IFN-β	Forward	CAGCAATTTTCAGTGTCAGAAGC
	Reverse	TCATCCTGTCCTTGAGGCAGT
ISG15	Forward	GAGCTAGAGCCTGCAGCAAT
	Reverse	TCACGGACACCAGGAAATCG
CXCL10	Forward	TGCCCTGACAAACTAATGAGC
	Reverse	CAAGGCATATTCTGCACCAG
IFIT2	Forward	ATGCCACTTCACCTGGAACC-
	Reverse	CTTCGGCTTCCCCTAAGCAT
LC3B	Forward	TGTCCGACTTATTCGAGAGCAGCA
	Reverse	TGTGTCCGTTCACCAACAGGAAGA
ATG5	Forward	GTGACTGGACTTACGGTGGG
	Reverse	GCCAAACTTCTTGCTCCCGA
ATG8	Forward	TCTGAGTCAAGAGGAGGGGT
	Reverse	CCGGGGCCGAAATAGCTTAG
ATG12	Forward	GCGAGCGGGTTCCCATT
	Reverse	CATTCCCAGCCATCGCCTAT
Beclin-1	Forward	TCAAGGCGTCACTTCTGGG
	Reverse	TTCTTTAGGCCCCGACGCTC
GAPDH	Forward	GGTGTGAACCATGAGAAGTATGA
	Reverse	GAGTCCTTCCACGATACCAAG
PEDV-N	Forward	GCAAAGACTGAACCCACTAAT
	Reverse	GCCTCTGTTGTTACTTGGAG

for 1 h. Protein signals were detected using an enhanced chemiluminescence (ECL) substrate (Beyotime, Shanghai, China) and an imaging system (Invitrogen iBright FL1500, Thermo Fisher Scientific, China). The experiment was performed in triplicate.

Transcriptome sequencing analysis

IPEC-J2 cells (1×10^6) were treated with LpEVs (10 μg/mL) for 12 h. Total RNA was then isolated from the cells via a RNeasy Mini Kit (QIAGEN, Hilden, Germany). Before downstream analysis, the integrity of the RNA was verified with a 2100 Bioanalyzer (Agilent Technologies, Palo Alto, CA, USA). Complementary DNA (cDNA) libraries were constructed following the manufacturer's instructions via the TruSeq stranded mRNA LT sample preparation kit (NEBNext® Ultra™ Directional RNA Library Prep Kit for Illumina®, NEB, USA). Clean reads were aligned rapidly and accurately to the reference genome with HISAT2 software to determine the read positioning information. Gene expression levels were quantified for each sample via the feature Counts tool in the subread software. Following the quantification of gene expression, statistical analysis was performed with DESeq to identify genes displaying significantly different expression levels under varying conditions. The criteria for selecting differentially expressed genes were defined as log2 (fold change) |> =1 and padj < = 0.05. Finally, gene ontology (GO) functional enrichment analysis and Kyoto Encyclopedia of Genes and Genomes (KEGG) pathway enrichment analysis were carried out on the differentially expressed gene set via cluster Profiler software, utilizing a threshold of padj < 0.05 for the analysis.

Autolysosome analysis

IPEC-J2 cells (5×10^5) seeded in 24-well plates were transfected with adenovirus encoding mCherry-GFP-LC3 (green fluorescence protein-red fluorescence protein-LC3) at an MOI of 10 for 24 h. Cells were exposed to LpEVs (2.5, 5, and 10 μg/mL) for an additional 12 h. Orange puncta displayed in mCherry-GFP-LC3-expressing cells are autophagosomes. Since the GFP signal is quenched in acidic lysosomes, red puncta represent autolysosomes, suggesting that cells undergo complete autophagy. Ten random fields per condition were analyzed in a blinded manner [31, 32]. Data shown as mean puncta/cell ± SD are representative of three independent experiments.

Treatment with inhibitors of autophagy and STING

To inhibit autophagy, cells were pretreated with 3-MA (5 mM in DMSO) for 3 h. After washing with PBS for three times, complete cell medium was supplemented with or without LpEVs (2.5 and 10 μg/mL) as described. Total Protein and RNA were extracted from treated cells at indicated time points for subsequent analysis.

To inhibit STING, cells were cultured in serum-free medium containing C-170 (1 μM) for 3 h. Residual C-170 was removed via washing with PBS for three times, and complete cell culture medium was supplemented with or without LpEVs (2.5 and 10 μg/mL) as described. Total Protein and RNA were extracted for subsequent analysis. Furthermore, autolysosome analysis was performed as described.

Cell treated with LpEVs and PEDV

IPEC-J2 cells (1×10^6) were treated with LpEVs at varying concentrations (2.5 and 10 μg/mL) at 37 °C for 12 h. After triple PBS washing to remove residual LpEVs, cells were infected with PEDV (MOI of 0.1) for 1 h. Unbound virions were eliminated through additional washing with PBS for three times. Infected cells were cultured in 2% FBS-maintenance medium at 37 °C for 24 h. Following 24 h incubation, total proteins were harvested to determine autophagic marked proteins by western blotting.

Determination of viral titers and replication in IPEC-J2 cells

IPEC-J2 cells were treated with LpEVs (2.5, 5 and 10 μg/mL) and PEDV (MOI of 0.1) as described. The viral suspension was harvested after three freeze–thaw cycles and subsequently quantified using the $TCID_{50}$ assay. In brief, cells (1×10^5 cells/well) in 96-well plates were inoculated with tenfold serial dilutions of viral sample. After 1 h incubation at 37 °C, the culture medium was replaced with fresh 2% FBS-maintenance medium. A tested in eight replicates. The cells were cultured until cytopathic effects (CPE), and $TCID_{50}$ was calculated using the Reed-Muench method. Furthermore, total RNA and protein extracts isolated from treated cells for parallel assessment of PEDV-N gene and protein expression using qPCR and western blotting, respectively.

Statistical analysis

All results are representative of three independent experiments. The data are presented as the mean ± standard error of the mean (SEM) and were analyzed with two-tailed Student's *t-tests* or one-way analysis of variance using GraphPad Prism 9.4.1 (GraphPad Software, USA). *P* values < 0.05 were considered to indicate statistical significance and are shown as $^{*}P < 0.05$, $^{**}P < 0.01$, $^{***}P < 0.001$, $^{****}P < 0.0001$.

Results

Lactiplantibacillus plantarum JL01 spontaneously releases EVs.

To ensure the successful isolation and purification of LpEVs from the culture supernatant, we employed nanoparticle tracking analysis (NTA) and transmission electron microscopy (TEM) for verification. NTA revealed a relatively smooth particle size detection curve, indicating high purity, with the diameter of LpEVs measuring approximately 132.5 nm and a yield of about 4.56×10^{10} particles per liter (Fig. 1 A, B). Additionally, TEM revealed that LpEVs exhibited a closed spherical lipid bilayer membrane structure (Fig. 1 C). Results of CCK8 demonstrated that 2.5, 5, 10 and 20 μg/mL of LpEVs did not affect the cell viability (Fig. 1 D). After treatment with LpEVs (2.5 μg/mL) for 3, 6, 9, and 12 h, cell viability remained almost the similar level with control group (CON) (Fig. 1 E). These results indicate that the purified LpEVs did not adversely affect the viability of IPEC-J2 cells.

LpEVs activated the cGAS-STING pathway

To determine whether LpEVs can activate the cGAS-STING pathway, IPEC-J2 cells (1×10^6) were pre-treated with LpEVs at concentrations of 2.5, 5, and 10 μg/mL for 12 h. The expression of key proteins in the cGAS-STING pathway was subsequently analyzed via Western blotting. Compared with the CON group, we found that 2.5, 5, and 10 μg/mL LpEVs significantly enhanced the expression of cGAS, STING and phosphorylated IRF3. Interestingly, compared to 2.5 μg/mL LpEVs, the concentration of 10 μg/mL LpEVs significantly decreased the expression of cGAS and STING, as well as phosphorylated IRF3 (Fig. 2A-D). Further, to assess the expression and transcription levels of IFN-α and IFN-β, both ELISA and qPCR analyses were conducted in this study. The results showed that 2.5, 5 and 10 μg/mL LpEVs all significantly increased the production of IFN-α and IFN-β in comparison to CON group. Whereas IFN-α and IFN-β in 10 μg/mL LpEVs-treatment both showed a significant decrease compared with 2.5 μg/mL-treatment (Fig. 2 E–H). The transcription of ISGs further validated the effect of LpEVs, indicating LpEVs (2.5, 5 and 10 μg/mL) significantly up-regulated the transcription of CXCL10, IFIT2 and ISG15. Compared with 2.5 μg/mL LpEVs-treatment, 10 μg/mL LpEVs showed notably less transcription (Fig. 2I-K). These results suggest that LpEVs activated the cGAS-STING pathway, with the effect appearing independent dosage manner.

LpEVs stimulate the transcription of various autophagy-related genes

We conducted a transcriptome analysis through RNA sequencing to investigate how high concentration (10 μg/mL) LpEVs influence cGAS-STING pathway. RNA sequencing was performed on three independent samples of IPEC-J2 cells. RNA-seq revealed that LpEVs led to the upregulation of 731 genes and the downregulation of 338 genes (Fig. 3A). A hierarchical clustering heatmap of the differentially expressed genes (DEGs) further illustrated the impact of LpEVs on gene expression variability among the replicates (Fig. 3B). Notably, Gene Ontology (GO) classification and Kyoto Encyclopedia of Genes and Genomes (KEGG) pathway analysis revealed that LpEVs treatment was significantly associated with the mitophagy pathway ($-\log10(padj) = 41$) (Fig. 3C). Further examination of the KEGG pathway diagram revealed that several autophagy-related genes, including LC3, ATG5, ATG9, NIX, Beclin-1, UB, and PINK1, were upregulated within this pathway (Fig. 3D). The results showed that 10 μg/mL LpEVs treatment could effectively stimulate the up-regulation of transcription of various autophagy-related genes in IPEC-J2 cells.

LpEVs induced autophagy in IPEC-J2 Cells

Based on KEGG enrichment analysis from transcriptomic sequencing, we investigated whether LpEVs-treatment can trigger autophagy in IPEC-J2 cells. The cells were treated with LpEVs as described above mentioned. The results showed that both 5 and 10 μg/mL LpEVs

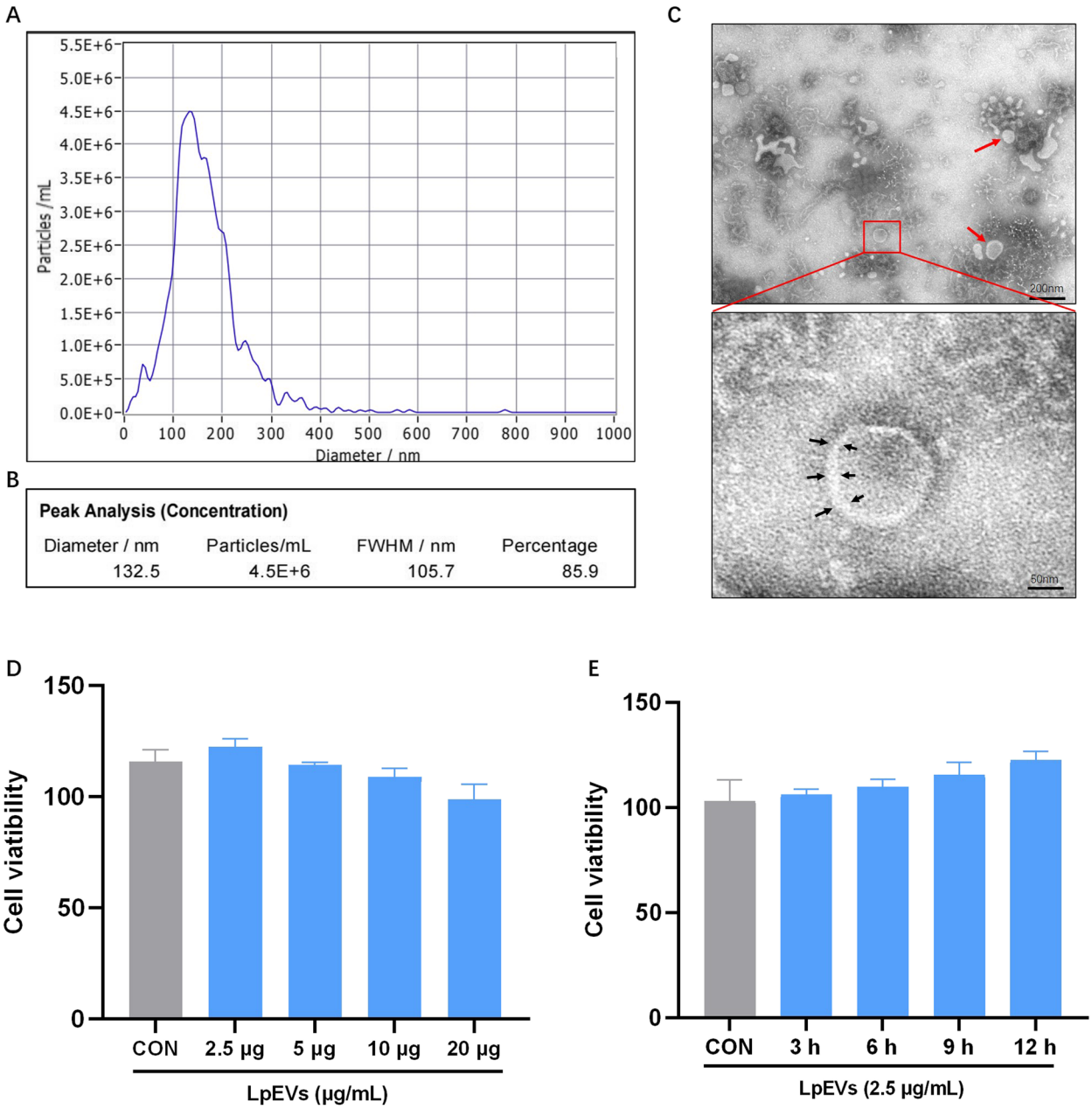

Fig. 1 Purification of EVs from *Lactiplantibacillus plantarum* JL01. **A**-**B** NTA analysis of purified LpEVs. **C** TEM images analysis of purified LpEVs. The profile of the LpEVs image is magnified, with the lipid bilayer indicated by black arrows. The black arrows on both sides indicate the potential bilayer of the vesicle. Scale bars: 200 nm (upper panel), 50 nm (lower panel). **D**, **E** Determination of cell viability with or without LpEVs treatment by CCK8. The results are presented as the means ± SEM of three repeats

significantly induced autophagy, as indicated by the conversion of LC3I to LC3II and the degradation of P62, compared to the control group. However, the effect of 2.5 μg/mL LpEVs on the induction of autophagy was not obvious via western blotting (Fig. 4A-C). qPCR results were consistent, revealing that 10 μg/mL LpEVs significantly upregulated the transcription of LC3B, ATG5, ATG8, ATG12, and Beclin-1 genes, whereas 2.5 μg/mL LpEVs did not showed such effect (Fig. 4D-H). Fluorescence microscopy was subsequently used to assess the ability of LpEVs to induce autophagosome-lysosome system formation. In non-autophagic cells, mCherry-GFP-LC3B appeared as diffuse orange fluorescence (a combination of mCherry and GFP) in the cytoplasm

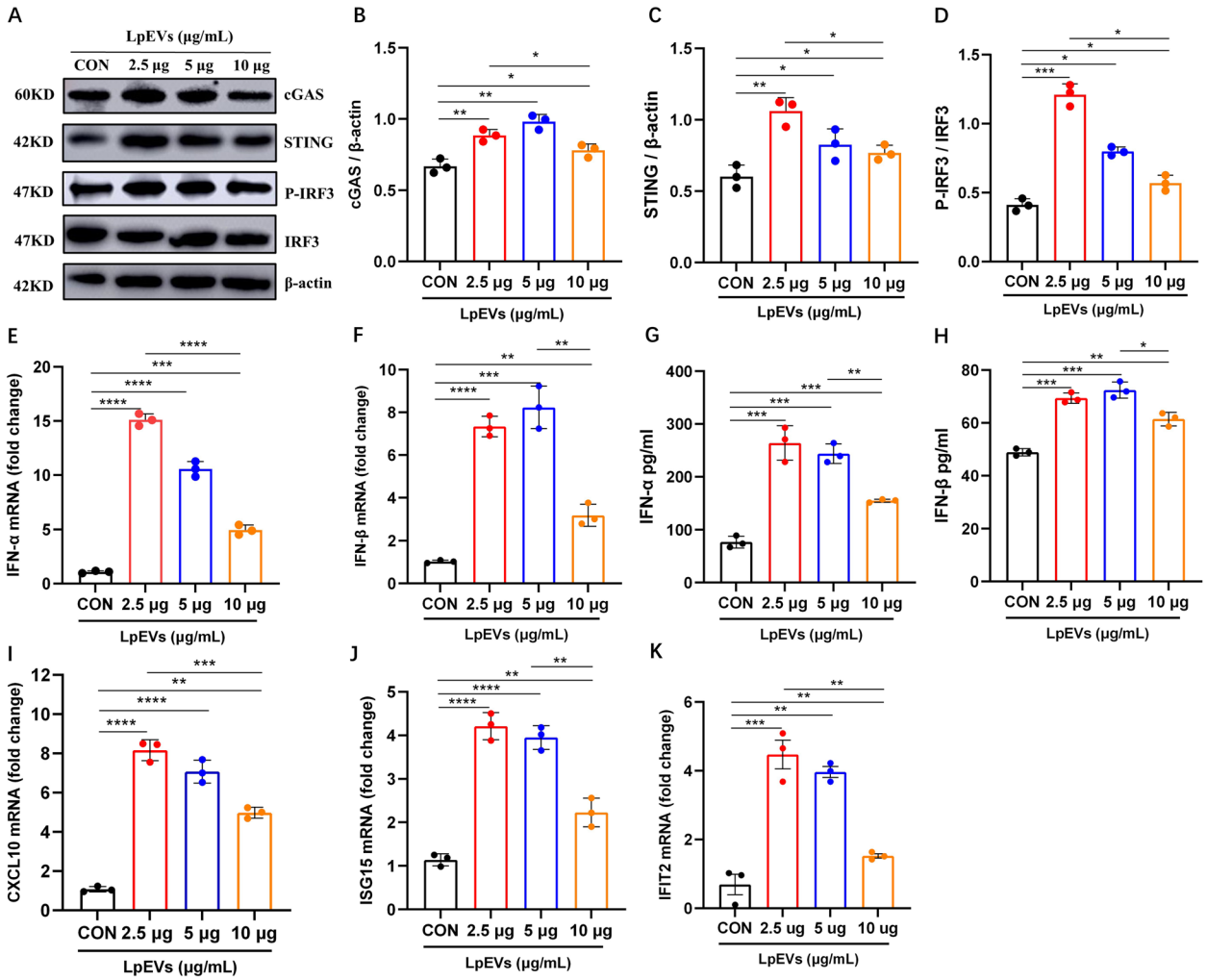

Fig. 2 Effects of LpEVs on the cGAS-STING pathway. IPEC-J2 cells (1×10^6) were treated with LpEVs at concentrations of 2.5, 5, and 10 μg/mL for 12 h. **A**-**D** Protein levels of cGAS, STING, and P-IRF3 were determined via western blotting. The ratios of cGAS/β-actin, STING/β-actin, and P-IRF3/IRF3 were analyzed via Image Studio Lite. **E**, **F** Transcription levels of IFN-α and IFN-β via qPCR. **G**, **H** Expression levels of IFN-α and β via ELISA. **I**-**K** Transcription levels of the interferon-stimulated genes (ISGs), including CXCL10, IFIT2, and ISG15 via qPCR. The results are presented as the means ± SEM of three repeats (*$P < 0.05$, **$P < 0.01$, ***$P < 0.001$, ****$P < 0.0001$)

under a fluorescence microscope. In autophagic cells, mCherry-GFP-LC3B aggregated on the autophagosome membrane, resulting in orange spots. After autophagosomes fused with lysosomes, the fluorescence of GFP was partially quenched, resulting in red spots, which indicated that the cells had undergone complete autophagy. As shown in Fig. 4I, J, diffuse orange fluorescence was observed in untreated IPEC-J2 cells (CON group). After treatment with 2.5 μg/mL LpEVs, there was a slight increase in orange spots compared with that in control. The cells treated by 5 μg/mL LpEVs significantly increased the number of red puncta. Moreover, almost entirely red puncta were observed in the cells treated with 10 μg/mL LpEVs. Collectively, these findings demonstrate that LpEVs trigger autophagic activation in IPEC-J2 cells at concentrations of 5 and 10 μg/mL.

LpEVs induced autophagy to limit excessive activation of cGAS-STING pathway

To determine whether LpEVs negatively regulate the cGAS-STING pathway via autophagy, IPEC-J2 (1×10^6) was added with autophagy inhibitor 3-MA and subsequently treated with LpEVs (2.5 and 10 μg/mL) as above mentioned. The result showed that 3-MA effectively decreased LC3-expression and the transcription of LC3B, enhanced P62-expression mediated by LpEVs (Fig. 5A-D). We subsequently examined activation of the cGAS-STING pathway. After the addition of 3-MA,

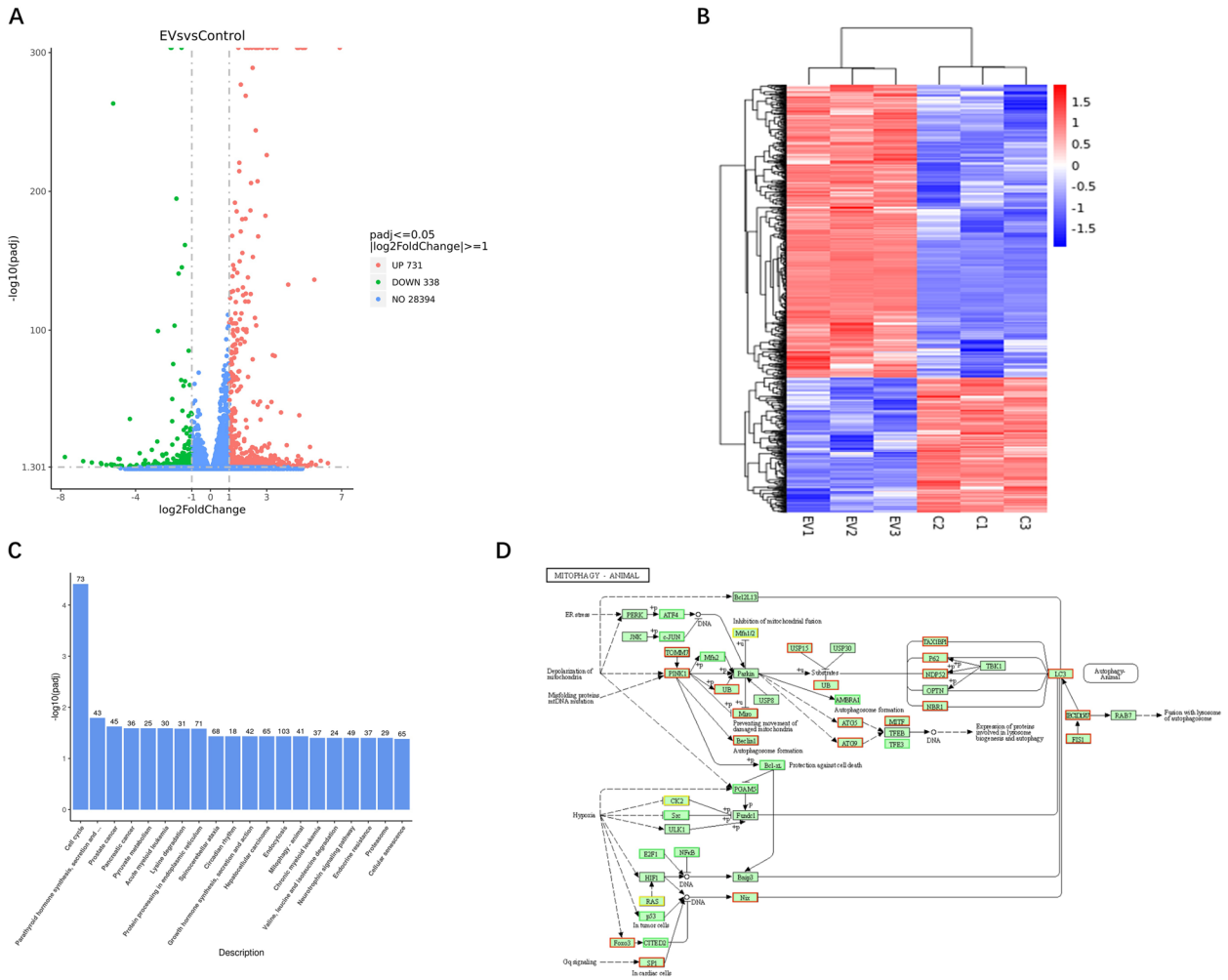

Fig. 3 Effects of LpEVs Treatment on Autophagy Genes in IPEC-J2 Cells. **A** Scatter plot of differentially expressed gene (DEG) analysis results. **B** Heatmap of significantly differentially expressed genes (DEGs) in each treatment sample after 12 h of LpEVs treatment. **C** KEGG analysis of DEGs in IPEC-J2 cells treated with LpEVs. KEGG pathway enrichment was considered significant when the p-value was less than 0.05, and the 20 most significant pathways are presented in a bar chart. **D** Analysis of upregulated and downregulated genes in the mitophagy pathway following LpEVs treatment

10 μg/mL LpEVs significantly increased the expression of cGAS, STING, and phosphorylated IRF3 to compare with the same dosage of LpEVs without 3-MA. However, 2.5 μg/mL LpEVs did not influence the expression of these proteins even with 3-MA (Fig. 5E-H). Furthermore, qPCR and ELISA demonstrated that 3-MA significantly increased the production of IFN-α/β mediated by 10 μg/mL LpEVs (Fig. 5I-L). Similarly, the transcription of CXCL10, IFIT2, and ISG15 revealed a similar trend (Fig. 5M-O). These indicate that the effect of 10 μg/mL LpEVs on the cGAS-STING pathway was reversed upon inhibiting autophagy. Therefore, higher doses of LpEVs (10 μg/mL) triggered autophagy to limit excessive activation of the cGAS-STING pathway.

STING played a crucial role in LpEVs-induced autophagy

To investigate whether LpEVs induce autophagy via STING, IPEC-J2 cells (1×10^6) were pretreated with the STING inhibitor C-170 and administrated with LpEVs. Results indicated that C-170 significantly inhibited STING expression (Fig. 6A, B). We subsequently assessed the expression of autophagy marker proteins via western blotting. The results indicated that the autophagy trigged by 10 μg/mL LpEVs was significantly suppressed upon C-170 pretreatment, evidenced by reduced conversion of LC3 I to LC3 II and P62 degradation, compared to that without C-170 (Fig. 6A, C, D). Consistently, the transcription of ATG5, ATG8, ATG12, and Beclin-1 induced by 10 μg/mL LpEVs was also significantly reduced after C-170 treatment

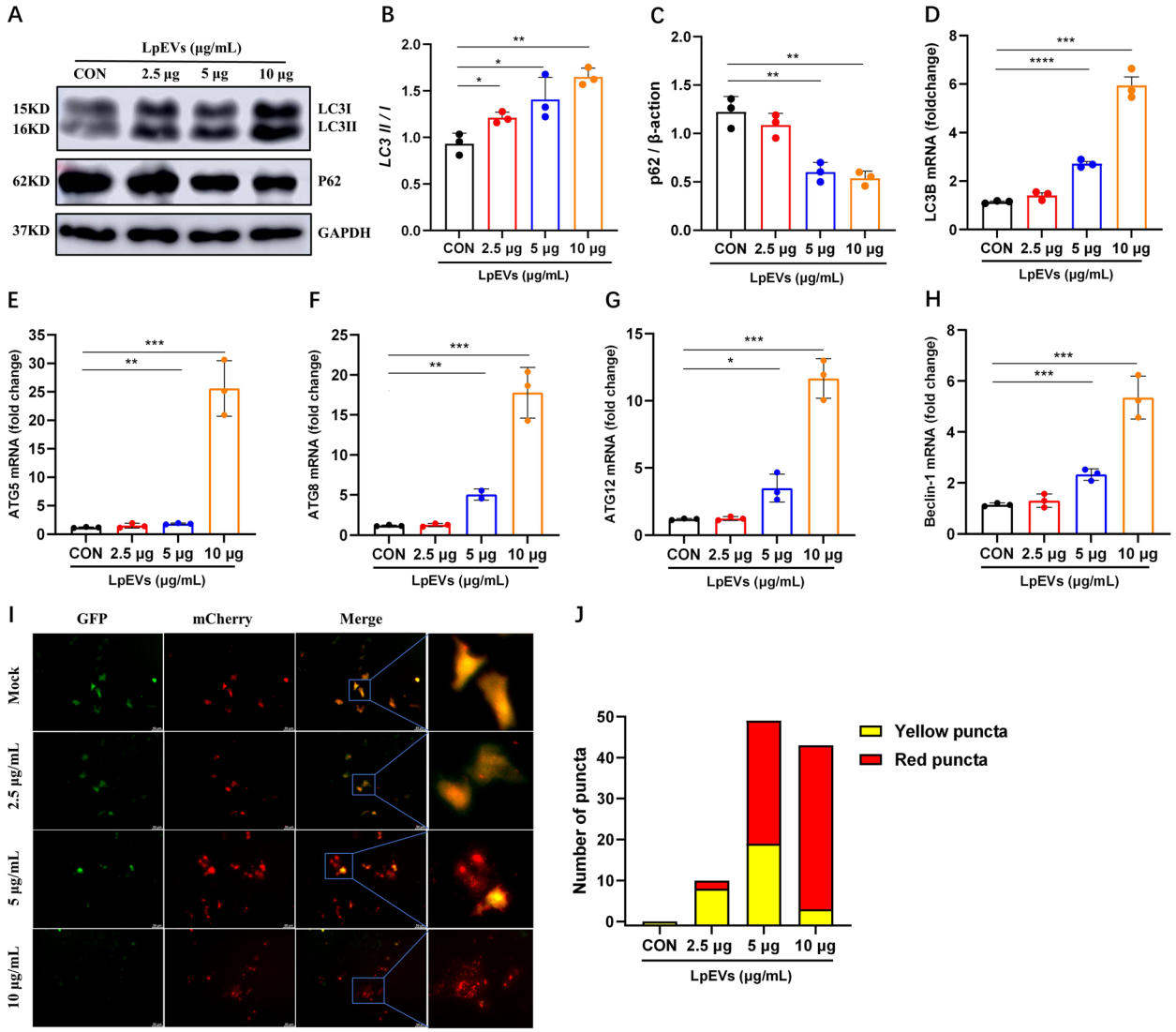

Fig. 4 Effects of LpEVs on autophagy in IPEC-J2 cells. IPEC-J2 cells (1×10^6) were treated with LpEVs at concentrations of 2.5, 5 and 10 μg/mL for 12 h, separately. **A**-**C** Protein levels of LC3 and P62 were analyzed, and Image Studio Lite was used to assess the ratios of LC3-II/LC3-I and P62/β-actin. **D**-**H** Transcription levels of the autophagy-related genes LC3B, ATG5, ATG8, ATG12 and Beclin-1 via qPCR. **I**, **J** IPEC-J2 cells transfected with mCherry-GFP-LC3B (MOI of 10) were examined under a fluorescence microscope for orange autophagosome spots and red autolysosome spots, and quantitative analysis was conducted. Scale bar, 50 μm. The results are presented as the means ± SEM of three repeats (*$P < 0.05$, **$P < 0.01$, ***$P < 0.001$)

(Fig. 6E-H). After the addition of C-170, autophagic lysosomes (red dots) in IPEC-J2 cells treated with 10 μg/mL LpEVs were significantly less than that without C-170, indicating that C-170 inhibited the formation of autophagic flux (Fig. 6I, J). These demonstrated STING plays a pivotal role in the process of autophagy triggered by LpEVs.

LpEVs induce autophagy to suppress PEDV replication in IPEC-J2 cells

To clarify the antiviral effects of different concentrations of LpEVs, we specifically investigated whether LpEVs-induced autophagy influenced PEDV proliferation. IPEC-J2 cells (1×10^6) were treated with LpEVs (2.5, 5 and 10 μg/mL) and infection with PEDV (MOI of 0.1). Results showed that LpEVs significantly inhibited the expression and transcription of N protein, as well as viral titer in a dose-dependent manner (Fig. 7A-D). In addition, we also observed PEDV increased the conversion of LC3 I to LC3 II, and degraded p62 significantly to compare with CON group. However, the effect of PEDV on activating autophagy was significantly lower than that observed in 10 μg/mL LpEVs + PEDV group, while

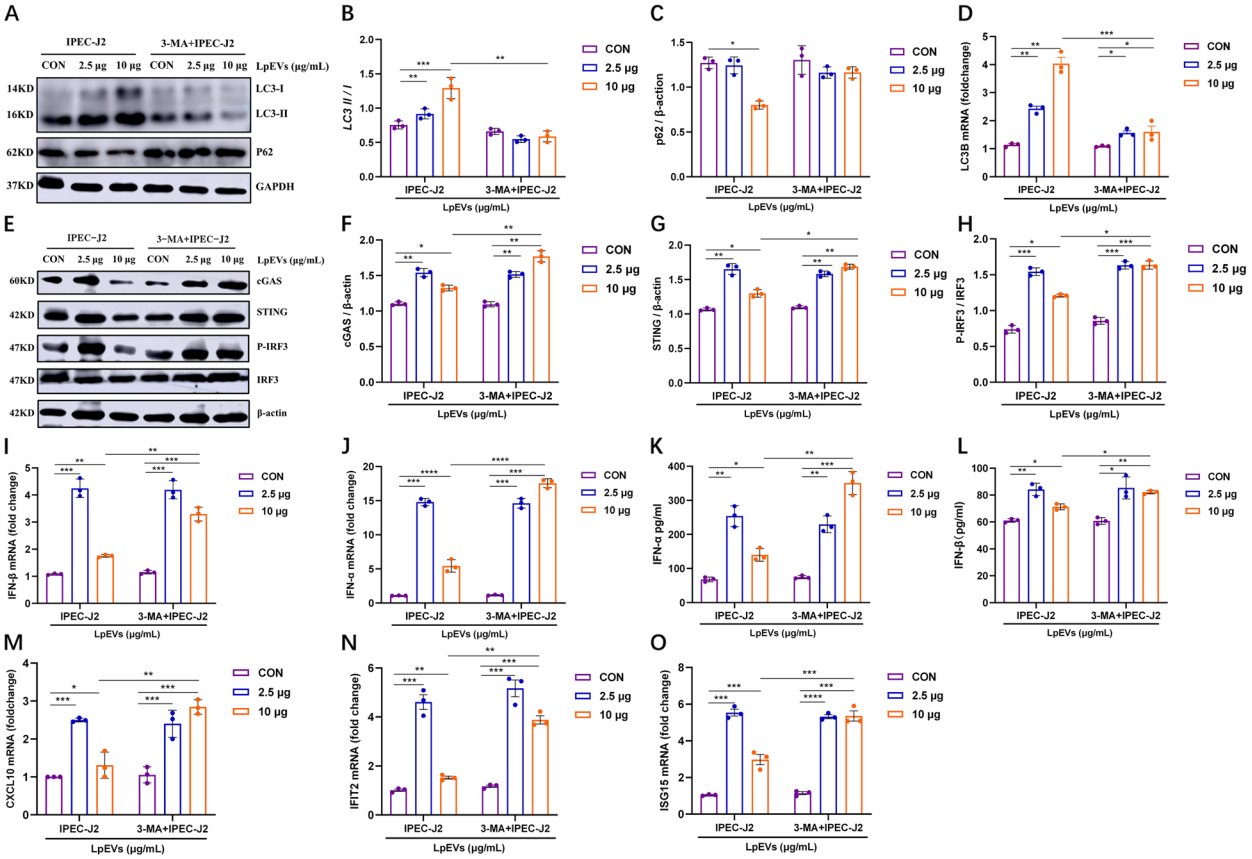

Fig. 5 LpEVs induced autophagy to limit the excessive activation of cGAS-STING pathway. IPEC-J2 cells (1×10^6) were pretreated with the autophagy inhibitor 3-MA (5 mM) for 3 h. Subsequently, the IPEC-J2 cells were treated with LpEVs at concentrations of 2.5 and 10 μg/mL for 12 h. **A**-**C** Protein levels of LC3 and P62 were analyzed, and Image Studio Lite was used to assess the ratios of LC3-II/LC3-I and P62/β-actin via western blotting. **D** Transcription level of LC3B via qPCR. **E**–**H** Expression levels of cGAS, STING, and phosphorylated proteins IRF3 were analyzed via Image Studio Lite to determine the ratios of cGAS/β-actin, STING/β-actin, or P-IRF3/IRF3. **I**, **J** Transcription levels of IFN-α and IFN-β via qPCR. (K, L) Secretion of IFN-α and IFN-β via ELISA. **M**–**O** Transcription levels of the interferon-stimulated genes (ISGs), including CXCL10, IFIT2, and ISG15. The results are presented as the means ± SEM of three repeats (*$P < 0.05$, **$P < 0.01$, ***$P < 0.001$, ****$P < 0.0001$)

being comparable to 2.5 μg/mL LpEVs + PEDV group (Fig. 7E-G).

To assess the antiviral effect of autophagy triggered by LpEVs, IPEC-J2 cells were pre-treated with 3-MA prior to treatment with LpEVs, as previously described. Our results indicated that the presence of 3-MA inhibited the antiviral effect of LpEVs, as demonstrated by an increase in the expression and transcription of N protein, as well as viral titer (Fig. 7H-K). These indicate that autophagy triggered by LpEVs enhances the antiviral effect, which is helpful to inhibit PEDV proliferation.

Discussion

Extracellular vesicles (EVs) derived from probiotics are believed to possess beneficial immunomodulatory properties, by conveying immune signals and modulating the activity of host cells [33]. Emerging evidence highlights their anti-viral properties by distinct molecular mechanism, which represent a paradigm shift in microbiome-based antiviral strategies [34, 35]. While early studies primarily attributed these effects to generic immunomodulation (TLR3 activation) or physical barrier enhancement, recent advances reveal strain-specific mechanisms operating at molecular, cellular, and systemic levels [36]. For example, EVs derived from *Enterobacter cloacae* and *Bacteroides thetaiotaomicron* significantly induce the gene expression of antiviral cytokines, including IL-6, TNF-α, IL-1β, and IFN-γ, thereby reduce murine norovirus replication in RAW264.7 cell [37].EVs derived from the beneficial commensal bacterium *Escherichia coli* Nissle 1917 can activate the cGAS-STING-type I interferon axis to promote the clearance of DNA viruses (herpes simplex virus type 1) and RNA viruses (vesicular stomatitis virus) in a cGAS-dependent manner [7]. In this study, we observed that LpEVs could modulate innate antiviral immunity via

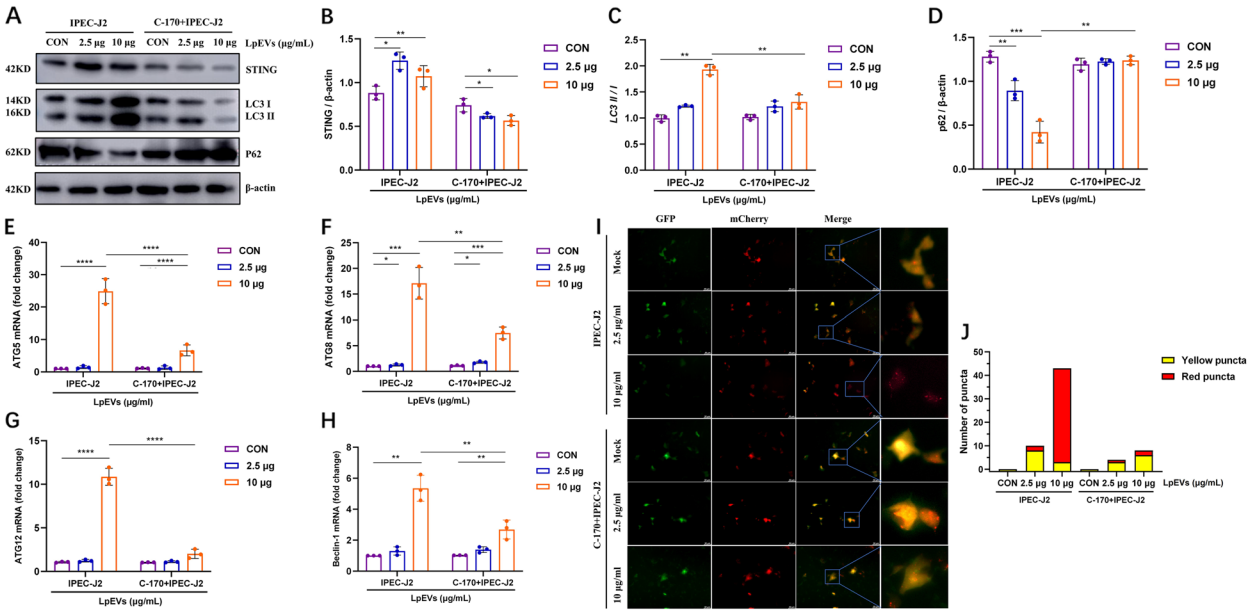

Fig. 6 STING played a crucial role in LpEVs-induced autophagy. IPEC-J2 cells ($1 \times 10.^{6}$) were pretreated with the STING inhibitor C-170 (1 μM) for 3 h. Subsequently, LpEVs at concentrations of 2.5, 5, and 10 μg/mL were added, and the IPEC-J2 cells were treated for 12 h. **A**-**D** Expression levels of STING, LC3, and P62 were analyzed, and Image Studio Lite was used to assess the ratios of STING/β-actin, LC3-II/LC3-I, and P62/β-actin. **E**–**H** Transcription levels of the autophagy-related genes ATG5, ATG8, ATG12, and Beclin-1. **I**, **J** IPEC-J2 cells transfected with mCherry-GFP-LC3B (MOI of 10). Quantitative analysis was conducted to examine the orange autophagosome spots and red autolysosome spots under a fluorescence microscope. The results are presented as the means ± SEM of three repeats (*$P < 0.05$, **$P < 0.01$, ***$P < 0.001$)

the cGAS-STING pathway in IPEC-J2 cells, as evidenced by increased levels of cGAS, STING, phospho-IRF3, IFN-α, IFN-β, and ISGs. This aligns with some previous study demonstrating that probiotic EVs activate cytosolic DNA-sensing machinery [38]. Interestingly, the activation of cGAS-STING pathway mediated by LpEVs was not in a dose-dependent manner. Higher doses (10 μg/mL) paradoxically suppressed cGAS-STING signaling and IFN responses compared to lower doses (2.5 μg/mL). Some studies demonstrated that 5 μg/mL of *Lactobacillus plantarum*-derived EVs could significantly increase TNF-α, IL-1β and IL-6, showing a strong immune effect. In contrast to lower doses, 10 μg/mL doses suppressed IL-1β and increased IL-10 secretion [39]. This biphasic regulation speculated a threshold-dependent mechanism, where excessive activation triggers negative feedback.

Emerging evidences demonstrate the cGAS-STING pathway as a pivotal regulator of autophagy, orchestrating both homeostatic cellular clearance and pathogen-directed immune responses. STING undergoes LC3 lipidation-dependent autophagic degradation via p62/SQSTM1 binding, forming a negative feedback loop to prevent hyperactivation [40]. In addition, STING mediated by the WD40 domain of ATG16L1, activates LC3 lipidation onto single-membrane perinuclear vesicles, thereby inducing autophagy [19]. In this study, we also observed that 10 μg/mL LpEVs significantly induced autophagy in IPEC-J2 cells, manifested by increased conversion of LC3 I to LC3 II, degradation of P62, marked upregulation of autophagy-related genes (ATG5, ATG8, ATG12, and Beclin-1), and formation of autophagic flux. To investigate whether the regulatory effects of high-dose LpEVs on the STING-IFN pathway are predominantly autophagy-dependent, we employed the autophagy inhibitor 3-methyladenine (3-MA). As a class III phosphatidylinositol 3-kinase (PI3 K) inhibitor, 3-MA exerts its autophagic suppression by blocking VPS34 catalytic activity [41]. The critical role of autophagy in tempering cGAS-STING over-activation was demonstrated through 3-MA inhibition experiments: autophagy inhibitor reversed the effect of 10 μg/mL LpEVs on regulation of cGAS-STING pathway. Notably, lower LpEVs doses (2.5 μg/mL) did not engage this regulatory loop, speculating autophagy-mediated suppression occurs only when immune stimulation exceeds a physiological threshold. Such dose-specific crosstalk highlights the precision of host-probiotic equilibrium.

To investigate whether STING is a pivotal mediator of LpEVs-induced autophagy, we utilized the covalent inhibitor STING-IN-2 (C-170), which specifically targets the transmembrane cysteine residue (Cys91) of STING. This small molecule irreversibly inhibits STING

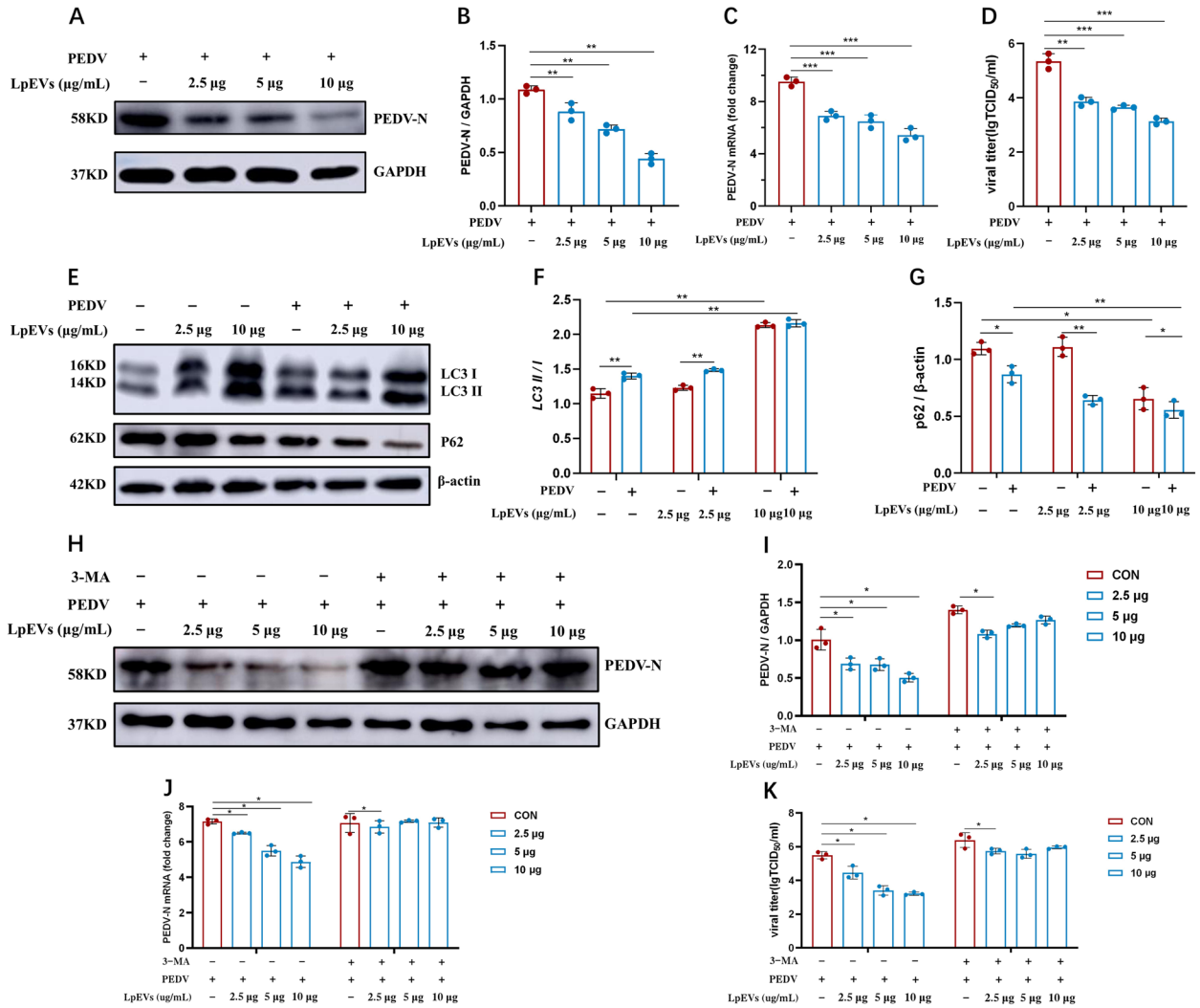

Fig. 7 LpEVs induce autophagy to suppress PEDV replication in IPEC-J2 cells. IPEC-J2 cells (1×10^6) were pretreated with the autophagy inhibitor 3-MA (5 mM) for 3 h. Subsequently, IPEC-J2 cells was treated with LpEVs at concentrations of 2.5, 5 and 10 μg/mL for 12 h, followed by challenged with PEDV (MOI of 0.1). **A**, **B** Levels of the PEDV-N protein was analyzed via Image Studio Lite to assess the ratio of PEDV-N/β-actin. **C** $TCID_{50}$ assay to detect the viral titer of PEDV in IPEC-J2 cells. **D** qPCR was used to detect the mRNA levels of PEDV-N gene. **E**–**G** The protein levels of LC3 and P62 were analyzed via Image Studio Lite to assess the ratios of LC3-II/LC3-I and P62/β-actin. **H**, **I** PEDV-N protein was analyzed via Image Studio Lite to assess the ratios of PEDV-N/β-actin with 3-MA. **J** $TCID_{50}$ assay to detect the viral titer of PEDV in IPEC-J2 cells with 3-MA. **K** qPCR was used to detect the mRNA levels of PEDV-N gene with 3-MA. The results are presented as the means ± SEM of three experiments (*$P < 0.05$, **$P < 0.01$, ***$P < 0.001$)

activation by preventing its functional conformational rearrangements and subsequent downstream signaling cascades [42]. C-170 treatment effectively attenuated LpEVs-induced autophagy at 10 μg/mL, as demonstrated by decreased LC3 II/LC3 I ratio, impaired P62 degradation, suppression of autophagic flux, and downregulation of autophagy-related gene expression. These indicate that STING is also essential in LpEVs-induced autophagy. This interdependent relationship between STING and autophagy reflects a conserved mechanism by which LpEVs balance immune defense and cellular homeostasis.

Interestingly, the resulting autophagy not only modulates the activity of the cGAS-STING pathway but also directly suppresses PEDV replication. Hopefully, LpEVs decreased PEDV-N protein expression and viral titers in a dose-dependent manner. Upon the addition of 3-MA, we observed that this antiviral effect disappeared, indicating that LpEVs limit PEDV proliferation in cells even though at the state of autophagy. These results were consistent with previous findings by Ko S. et al. regarding the induction of autophagy in IPEC-J2 cells ultimately inhibiting PEDV proliferation [26]. This dual role-suppressing

excessive inflammation while enhancing antiviral effector functions-positions autophagy as a central coordinator of LpEVs-mediated protection.

In summary, our study elucidates that LpEVs activate the cGAS-STING pathway and induce autophagy in IPEC-J2 cells. Furthermore, LpEVs engage autophagy to restrict excessive activation of this pathway while suppressing intracellular proliferation of PEDV. Notably, STING-mediated autophagy amplifies the antiviral efficacy of LpEVs. These findings lay a theoretical foundation for developing EV-based targeted antiviral strategies.

Supplementary Information

The online version contains supplementary material available at https://doi.org/10.1186/s12866-025-04019-y.

Supplementary Material 1.

Authors' contributions

C.W. and J.H. designed the experiments. S.Z. performed research and wrote the paper. X.S. organized and typeset the images. Q.G., A.S., J.X. and Q.L. helped with sample collection and data presentation. Z.L., Y.W. and X.Z. analyzed the data. X.C., Y.Z. and J.W. helped revise the manuscript. All authors read and approved the final manuscript.

Funding

This work was supported by the Jilin Province Science and Technology Project (20240601058RC). National Natural Science Foundation of China (U21 A20261, 32273043). Jilin province college students'innovation and entrepreneurship training program project (S202310193135, s202410193009).

Data availability

The sequence data supporting the results of this study were submitted to NCBI (NCBI, Bethesda, USA) with accession number PRJNA1175833. The specific link is https://www.ncbi.nlm.nih.gov/bioproject/?term=PRJNA1175833.

Declarations

Ethics approval and consent to participate

Not applicable.

Consent for publication

Not applicable.

Competing interests

The authors declare no competing interests.

Received: 8 December 2024 Accepted: 2 May 2025
Published online: 07 May 2025

References

1. Jung K, Saif LJ, Wang Q. Porcine epidemic diarrhea virus (PEDV): an update on etiology, transmission, pathogenesis, and prevention and control. Virus Res. 2020;286:198045.
2. Choudhury B, Dastjerdi A, Doyle N, Frossard JP, Steinbach F. From the field to the lab - an European view on the global spread of PEDV. Virus Res. 2016;226:40–9.
3. Watanabe T, Hayashi K, Kan T, Ohwaki M, Kawahara T. Anti-Influenza virus effects of Enterococcus faecalis KH2 and Lactobacillus plantarum SNK12 RNA. Biosci Microbiota Food Health. 2021;40(1):43–9.
4. Lu S, He S, Yue K, Mi J, Huang Y, Song L, Yang T, Ren Z, Ren L, Xu J. Lactobacillus plantarum GUANKE modulate anti-viral function of dendritic cells in mice. Int Immunopharmacol. 2024;15(134):112169.
5. Noda M, Danshiitsoodol N, Sakaguchi T, Kanno K, Sugiyama M. Exopolysaccharide Produced by Plant-Derived Lactobacillus plantarum SN35N Exhibits Antiviral Activity. Biol Pharm Bull. 2021;44(12):1886–90.
6. Olivo-Martínez Y, Martínez-Ruiz S, Cordero-Alday C, et al. Modulation of Serotonin-Related Genes by Extracellular Vesicles of the Probiotic Escherichia coli Nissle 1917 in the Interleukin-1β-Induced Inflammation Model of Intestinal Epithelial Cells. Int J Mol Sci. 2024;25(10):5338–5338.
7. Erttmann SF, Swacha P, Aung KM, et al. The gut microbiota prime systemic antiviral immunity via the cGAS-STING-IFN-I axis. Immunity. 2022;55(5):847-861.e10.
8. Liu Y, Defourny KAY, Smid EJ, et al. Gram-positive bacterial extracellular vesicles and their impact on health and disease. Front Microbiol. 2018;9:1502.
9. Grande R, Celia C, Mincione G, et al. Detection and physicochemical characterization of membrane vesicles (MVs) of lactobacillus reuteri DSM 17938. Front Microbiol. 2017;8:1040.
10. Li M, Lee K, Hsu M, et al. Lactobacillus-derived extracellular vesicles enhance host immune responses against vancomycin-resistant enterococci. BMC Microbiol. 2017;17(1):66.
11. Tong J, Song J, Zhang W, Zhai J, Guan Q, Wang H, Liu G, Zheng C. When DNA-damage responses meet innate and adaptive immunity. Cell Mol Life Sci. 2024;81(1):185.
12. He M, Jiang H, Li S, Xue M, Wang H, Zheng C, Tong J. The crosstalk between DNA-damage responses and innate immunity. Int Immunopharmacol. 2024;25(140):112768.
13. Sun L, Wu J, Du F, Chen X, Chen ZJ. Cyclic GMP-AMP synthase is a cytosolic DNA sensor that activates the type I interferon pathway. Science. 2013;339:786–91.
14. Hopfner KP, Hornung V. Molecular mechanisms and cellular functions of cGAS-STING signalling. Nat Rev Mol Cell Biol. 2020;21:501–21.
15. Liang Q, Seo GJ, Choi YJ, Kwak MJ, Ge J, Rodgers MA, Shi M, Leslie BJ, Hopfner KP, Ha T, et al. Crosstalk between the cGAS DNA sensor and Beclin-1 autophagy protein shapes innate antimicrobial immune responses. Cell Host Microbe. 2014;15:228–38.
16. Hang R, Kang R, Tang D. The STING1 network regulates autophagy and cell death. Signal Transduct Target Ther. 2021;6:208.
17. Pang Y, Wu L, Tang C, Wang H, Wei Y. Autophagy-Inflammation Interplay During Infection: Balancing Pathogen Clearance and Host Inflammation. Front Pharmacol. 2022;22(13):832750.
18. Liu D, Wu H, Wang C, Li Y, Tian H, Siraj S, et al. STING directly activates autophagy to tune the innate immune response. Cell Death Differ. 2019;26:1735–49.
19. Fischer TD, Wang C, Padman BS, Lazarou M, Youle RJ. STING induces LC3B lipidation onto single-membrane vesicles via the V-ATPase and ATG16L1-WD40 domain. J Cell Biol. 2020;219:e202009128.
20. Sun Y, Yu S, Ding N, Meng C, Meng S, Zhang S, et al. Autophagy Benefits the Replication of Newcastle Disease Virus in Chicken Cells and Tissues. J Virol. 2014;88:525–37.
21. Wang R, Zhu Y, Zhao J, Ren C, Li P, Chen H, et al. Autophagy Promotes Replication of Influenza A Virus In Vitro. J Virol. 2019;93:e01984-e2018.
22. Jin M, Zhang Y. Autophagy and inflammatory diseases. Adv Exp Med Biol. 2020;1207:391–400.
23. Chu P, He L, Huang R, et al. Autophagy Inhibits Grass Carp Reovirus (GCRV) Replication and Protects Ctenopharyngodon idella Kidney (CIK) Cells from Excessive Inflammatory Responses after GCRV Infection. Biomolecules. 2020;10(9):1296–1296.
24. Xia N, Zheng W, Jiang S, Cao Q, Luo J, Zhang J, Xu Y, Sun S, Zhang K, Chen N, Meurens F, Zhu J. Porcine cGAS-STING signaling induced autophagy inhibits STING downstream IFN and apoptosis. Front Immunol. 2022;13(13):1021384.
25. Liang S, Yun-Shan W, Li Dong-Yi, et al. Autophagy in Viral Infection and Pathogenesis. Front Cell Dev Biol. 2021;9:766142. https://doi.org/10.3389/fcell.2021.766142.
26. Ko S, Gu MJ, Kim CG, Kye YC, Lim Y, Lee JE, et al. Rapamycin-Induced Autophagy Restricts Porcine Epidemic Diarrhea Virus Infectivity in Porcine Intestinal Epithelial Cells. Antiviral Res. 2017;146:86–95.

27. Wang X, Tong W, Yang X, et al. RBM14 inhibits the replication of porcine epidemic diarrhea virus by recruiting p62 to degrade nucleocapsid protein through the activation of autophagy and interferon pathway. J Virol. 2024;98(3):e0018224.
28. Wang C, Zhang Y, Yang S, et al. Zn2+ inhibits PEDV replication by inducing autophagy through the Akt-mTOR pathway [J]. Vet Microbiol. 2025;301:110343.
29. Lee HK, Lund JM, Ramanathan B, et al. Autophagy-dependent viral recognition by plasmacytoid dendritic cells [J]. Science. 2007;315(5817):1398–401.
30. Liu RH, Sun AQ, Liao Y, Tang ZX, Zhang SH, Shan X, Hu JT. *Lactiplantibacillus plantarum* Regulated Intestinal Microbial Community and Cytokines to Inhibit Salmonella typhimurium Infection. Probiotics Antimicrob Proteins. 2023;15(5):1355–70.
31. Zhang J, Ruan T, Sheng T, et al. Role of c-Jun terminal kinase (JNK) activation in influenza a virus-induced autophagy and replication. Virology. 2019;526:1–12.
32. Wang J, Kan X, Li X, et al. Porcine epidemic diarrhoea virus (PEDV) infection activates AMPK and JNK through TAK1 to induce autophagy and enhance virus replication. Virulence. 2022;13(1):1697–712.
33. Molina-Tijeras JA, Galvez J, Rodriguez-Cabezas ME. The immunomodulatory properties of extracellular vesicles derived from probiotics: a novel approach for the management of gastrointestinal diseases. Nutrients. 2019;11(5):1038.
34. Chon J-W, Seo K-H, Kim Y-S, et al. Antiviral Effect of Probiotics against Respiratory Tract Infections: A Review. Journal of dairy science and biotechnology. 2023;41(2):57–66.
35. Wang H, Zhao Y, Pei Z, et al. Effect of Mixed Probiotics on Alleviating H1N1 Influenza Infection and Regulating Gut Microbiota. Foods. 2024;13(19):3079–3079.
36. Elean M, Albarracín L, Fukuyama K, et al. Lactobacillus delbrueckii CRL 581 Differentially Modulates TLR3-Triggered Antiviral Innate Immune Response in Intestinal Epithelial Cells and Macrophages. Microorganisms. 2021;9(12):2449–2449.
37. Bhar S, Zhao G, Bartel JD, Sterchele H, Del Mazo A, Emerson LE, Edelmann MJ, Jones MK. Bacterial extracellular vesicles control murine norovirus infection through modulation of antiviral immune responses. Front Immunol. 2022;13:909949.
38. Pan M, Yin Y, Tongyu Hu, et al. UXT attenuates the CGAS-STING1 signaling by targeting STING1 for autophagic degradation. Autophagy. 2022;19(2):440–56.
39. Kim SH, Lee JH, Kim EH, et al. Immunomodulatory Activity of Extracellular Vesicles of Kimchi-Derived Lactic Acid Bacteria (Leuconostoc mesenteroides, Latilactobacillus curvatus, and Lactiplantibacillus plantarum). Foods. 2022;11(3):313–313.
40. Prabakaran T, Bodda C, Krapp C, et al. Attenuation of cGAS-STING signaling is mediated by a p62/SQSTM1-dependent autophagy pathway activated by TBK1 [J]. EMBO J. 2018;37(8):e97858.
41. Zhang X, Wang H, Miao Yu, et al. Inhibition of autophagy by 3-methyladenine promotes migration and invasion of colon cancer cells through epithelial mesenchymal transformation. Translational cancer research. 2022;11(8):2834–42.
42. Haag SM, Gulen MF, Reymond L, et al. Targeting STING with covalent small-molecule inhibitors. Nature. 2018;559(7713):269–73.

Publisher's Note